

# Very High Energy Observations of Gamma-Ray Burst Locations with the Whipple Telescope

D. Horan<sup>1,7</sup>, R. W. Atkins<sup>2</sup>, H. M. Badran<sup>3</sup>, G. Blaylock<sup>4</sup>, S. M. Bradbury<sup>5</sup>, J. H. Buckley<sup>6</sup>, K. L. Byrum<sup>7</sup>, O. Celik<sup>8</sup>, Y. C. K. Chow<sup>8</sup>, P. Cogan<sup>9</sup>, W. Cui<sup>10</sup>, M. K. Daniel<sup>9</sup>, I. de la Calle Perez<sup>11</sup>, C. Dowdall<sup>9</sup>, A. D. Falcone<sup>12</sup>, D. J. Fegan<sup>9</sup>, S. J. Fegan<sup>8</sup>, J. P. Finley<sup>10</sup>, P. Fortin<sup>13</sup>, L. F. Fortson<sup>14</sup>, G. H. Gillanders<sup>15</sup>, J. Grube<sup>5</sup>, K. J. Gutierrez<sup>6</sup>, J. Hall<sup>2</sup>, D. Hanna<sup>16</sup>, J. Holder<sup>5</sup>, S. B. Hughes<sup>6</sup>, T. B. Humensky<sup>17</sup>, G. E. Kenny<sup>15</sup>, M. Kertzman<sup>18</sup>, D. B. Kieda<sup>2</sup>, J. Kildea<sup>16</sup>, H. Krawczynski<sup>6</sup>, F. Krennrich<sup>19</sup>, M. J. Lang<sup>15</sup>, S. LeBohec<sup>2</sup>, G. Maier<sup>5</sup>, P. Moriarty<sup>20</sup>, T. Nagai<sup>19</sup>, R. A. Ong<sup>8</sup>, J. S. Perkins<sup>6</sup>, D. Petry<sup>21</sup>, J. Quinn<sup>9</sup>, M. Quinn<sup>20</sup>, K. Ragan<sup>16</sup>, P. T. Reynolds<sup>22</sup>, H. J. Rose<sup>5</sup>, M. Schroedter<sup>19</sup>, G. H. Sembroski<sup>10</sup>, D. Steele<sup>14</sup>, S. P. Swordy<sup>17</sup>, J. A. Toner<sup>15</sup>, L. Valcarcel<sup>16</sup>, V. V. Vassiliev<sup>8</sup>, R. G. Wagner<sup>7</sup>, S. P. Wakely<sup>17</sup>, T. C. Weekes<sup>1</sup>, R. J. White<sup>5</sup>, D. A. Williams<sup>23</sup>

deirdreh@hep.anl.gov

## ABSTRACT

Gamma-ray burst (GRB) observations at very high energies (VHE,  $E > 100$  GeV) can impose tight constraints on some GRB emission models. Many

---

<sup>1</sup>Fred Lawrence Whipple Observatory, Harvard-Smithsonian Center for Astrophysics, P.O. Box 97, Amado, AZ 85645-0097

<sup>2</sup>Physics Department, University of Utah, Salt Lake City, UT 84112, USA

<sup>3</sup>Department of Physics, Tanta University, Tanta, Egypt

<sup>4</sup>Department of Physics, University of Massachusetts, Amherst, MA 01003-4525, USA

<sup>5</sup>School of Physics and Astronomy, University of Leeds, Leeds, LS2 9JT, UK

<sup>6</sup>Department of Physics, Washington University, St. Louis, MO 63130, USA

<sup>7</sup>Argonne National Laboratory, 9700 S. Cass Avenue, Argonne, IL 60439, USA

<sup>8</sup>Department of Physics and Astronomy, University of California, Los Angeles, CA 90095, USA

<sup>9</sup>School of Physics, University College Dublin, Belfield, Dublin 4, Ireland

<sup>10</sup>Department of Physics, Purdue University, West Lafayette, IN 47907, USA

<sup>11</sup>Department of Physics, University of Oxford, Oxford, OX1 3RH, UK

<sup>12</sup>Department of Astronomy and Astrophysics, 525 Davey Lab., Penn. State University, University Park, PA 16802, USA

<sup>13</sup>Department of Physics and Astronomy, Barnard College, Columbia University, NY 10027, USA

<sup>14</sup>Astronomy Department, Adler Planetarium and Astronomy Museum, Chicago, IL 60605, USA

<sup>15</sup>Physics Department, National University of Ireland, Galway, Ireland

<sup>16</sup>Physics Department, McGill University, Montreal, QC H3A 2T8, Canada

<sup>17</sup>Enrico Fermi Institute, University of Chicago, Chicago, IL 60637, USA

<sup>18</sup>Department of Physics and Astronomy, DePauw University, Greencastle, IN 46135-0037, USA

<sup>19</sup>Department of Physics and Astronomy, Iowa State University, Ames, IA 50011, USA

<sup>20</sup>Department of Physical and Life Sciences, Galway-Mayo Institute of Technology, Dublin Road, Galway, Ireland

<sup>21</sup>N.A.S.A./Goddard Space-Flight Center, Code 661, Greenbelt, MD 20771, USA

<sup>22</sup>Department of Applied Physics and Instrumentation, Cork Institute of Technology, Bishopstown, Cork, Ireland

<sup>23</sup>Santa Cruz Institute for Particle Physics and Department of Physics, University of California, Santa Cruz, CA 95064, USA

GRB afterglow models predict a VHE component similar to that seen in blazars and plerions, in which the GRB spectral energy distribution has a double-peaked shape extending into the VHE regime. VHE emission coincident with delayed X-ray flare emission has also been predicted. GRB follow-up observations have had high priority in the observing program at the Whipple 10 m Gamma-ray Telescope and GRBs will continue to be high priority targets as the next generation observatory, VERITAS, comes on-line. Upper limits on the VHE emission, at late times ( $> \sim 4$  hours), from seven GRBs observed with the Whipple Telescope are reported here.

*Subject headings:* gamma rays: bursts — gamma rays: observations

## 1. Introduction

Since their discovery in 1969 (Klebesadel, Strong & Olsen 1973), gamma-ray bursts (GRBs) have been well studied at many wavelengths. Although various open questions remain on their nature, there is almost universal agreement that the basic mechanism is an expanding relativistic fireball, that the radiation is beamed, that the prompt emission is due to internal shocks and that the afterglow arises from external shocks. It is likely that Lorentz factors of a few hundred are involved, with the radiating particles, either electrons or protons, being accelerated to very high energies. GRBs are sub-classified into two categories, long and short bursts, based on the timescale over which 90% of the prompt gamma-ray emission is detected.

Recently, the Swift GRB Explorer (Gehrels et al. 2004) has revealed that many GRBs have associated X-ray flares (Burrows et al. 2005; Falcone et al. 2006a). These flares have been detected between  $10^2$  s and  $10^5$  s after the initial prompt emission and have been found to have fluences ranging from a small fraction of, up to a value comparable to, that contained in the prompt GRB emission. This X-ray flare emission has been postulated to arise from a number of different scenarios, including late central engine activity where the GRB progenitor remains active for some time after, or re-activates after, the initial explosion (Kumar & Piran 2000; Zhang et al. 2006; Nousek et al. 2006; Perna et al. 2005; Proga & Zhang 2006; King et al. 2005) and refreshed shocks which occur when slower moving shells ejected by the central engine in the prompt phase catch up with the afterglow shock at late times (Rees & Mészáros 1998; Sari & Mészáros 2000; Granot, Nakar & Piran 2003; Guetta et al. 2006). For short GRBs, shock heating of a binary stellar companion has also been proposed (MacFadyen, Ramirez-Ruiz & Zhang 2005). It is not yet clear whether the X-ray flares are the result of prolonged central engine activity, refreshed shocks or some other

mechanism (Panaitescu et al. 2006). A very high energy (VHE;  $E > 100$  GeV) component of this X-ray flare emission has also been predicted (Wang, Li & Mészáros 2006).

Within the standard fireball shock scenario (Rees & Mészáros 1992; Mészáros & Rees 1993; Sari, Piran & Narayan 1998), many models have been proposed which predict emission at and above GeV energies during both the prompt and afterglow phases of the GRB. These have been summarized by Zhang & Mészáros (2004), and references therein, and include leptonic models in which gamma rays are produced by electron self-inverse-Compton emission from the internal shocks or from the external forward or reverse shocks. Other models predict gamma rays from proton synchrotron emission or photomeson cascade emission in the external shock or from a combination of proton synchrotron emission and photomeson cascade emission from internal shocks.

Although GRB observations are an important component of the program at many VHE observatories, correlated observations at these short wavelengths remain sparse even though tantalizing and inherently very important. The sparsity of observations of GRBs at energies above 10 MeV is dictated not by lack of interest in such phenomena, or the absence of theoretical predictions that the emission should occur, but by the experimental difficulties.

For the observation of photons of energies above 100 GeV, only ground-based telescopes are available at present. These ground-based telescopes fall into two broad categories, air shower arrays and atmospheric Cherenkov telescopes (of which the majority are Imaging Atmospheric Cherenkov Telescopes, or IACTs). The air shower arrays, which have wide fields of view making them particularly suitable for GRB searches, are relatively insensitive. There are several reports from these instruments of possible TeV emission. Padilla et al. (1998) reported possible VHE emission at  $E > 16$  TeV from GRB 920925c. While finding no individual burst which is statistically significant, the Tibet-AS $\gamma$  Collaboration found an indication of 10 TeV emission in a stacked analysis of 57 bursts (Amenomori et al. 2001). The Milagro Collaboration reported on the detection of an excess gamma-ray signal during the prompt phase of GRB 970417a with the Milagrito detector (Atkins et al. 2000). In all of these cases however, the statistical significance of the detection is not high enough to be conclusive. In addition to searching the Milagro data for VHE counterparts for 25 satellite-triggered GRBs (Atkins et al. 2005), the Milagro Collaboration conducted a search for VHE transients of 40 seconds to 3 hours duration in the northern sky (Atkins et al. 2004). No evidence for VHE emission was found from either of these searches and upper limits on the VHE emission from GRBs were derived. Atmospheric Cherenkov telescopes, particularly those that utilize the imaging technique, are inherently more flux-sensitive than air shower arrays and have better energy resolution but are limited by their small fields of view (3-5°) and low duty cycle ( $\sim 7\%$ ). In the Burst And Transient Source Explorer (Meegan et al. 1992)

era (1991-2000), attempts at GRB monitoring were limited by slew times and uncertainty in the GRB source position (Connaughton et al. 1997).

Swift, the first of the next generation of gamma-ray satellites which will include AGILE (Astro-rivelatore Gamma a Immagini LEggero) and the Gamma-ray Large Area Space Telescope (GLAST), is beginning to provide arcminute localizations so that IACTs are no longer required to scan a large GRB error box in order to achieve full coverage of the possible emission region. The work in this paper covers the time period prior to the launch of the Swift satellite.

The minimum detectable fluence with an IACT, such as the Whipple 10m, in a ten second integration is  $< 10^{-8}$  erg cm $^{-2}$  (5 photons of 300 GeV in  $5 \times 10^8$  cm $^2$  collection area). This is a factor of  $> 100$  better than GLAST will achieve (3 photons of 10 GeV in  $10^4$  cm $^2$  collection area). This ignores the large solid angle advantage of a space telescope and the possible steepening of the observable spectrum because of the inherent emission mechanism and the effect of intergalactic absorption by pair production. There have been many predictions of high energy GRB emission in and above the GeV energy range (Mészáros, Rees, & Papathanassiou 1994; Boettcher & Dermer 1998; Pilla & Loeb 1998; Wang, Dai & Lu 2001; Zhang & Mészáros 2001; Guetta & Granot 2003b; Dermer & Atoyan 2004; Fragile et al. 2004); also see Zhang & Mészáros (2004) and references therein.

Until AGILE and GLAST are launched, the GRB observations that were made by the EGRET experiment on the Compton Gamma Ray Observatory (CGRO) will remain the most constraining in the energy range from 30 MeV to 30 GeV. Although EGRET was limited by a small collection area and large dead time for GRB detection, it made sufficient detections to indicate that there is a prompt component with a hard spectrum that extends at least to 100 MeV energies. The average spectrum of four bursts detected by EGRET (GRBs 910503, 930131, 940217 & 940301) did not show any evidence for a cutoff up to 10 GeV (Dingus 2001). The relative insensitivity of EGRET was such that it was not possible to eliminate the possibility that all GRBs had hard components (Dingus, Catelli & Schneid 1998). EGRET also detected an afterglow component from GRB 940217 that extended to 18 GeV for at least 1.5 hours after the prompt emission indicating that a high-energy spectral component can extend into the GeV band for a long period of time, at least for some GRBs (Hurley et al. 1994). The spectral slope of this component is sufficiently flat that its detection at still higher energies may be possible (Mannheim, Hartmann & Funk 1996). Mészáros & Rees (1994) attribute this emission to the combination of prompt MeV radiation from internal shocks with a more prolonged GeV inverse Compton component from external shocks. It is also postulated that this emission could be the result of inverse Compton scattering of X-ray flare photons (Wang, Li & Mészáros 2006). Although somewhat extreme parameters must

be assumed, synchrotron self-Compton emission from the reverse shock is cited as the best candidate for this GeV emission by Granot & Guetta (2003), given the spectral slope that was recorded. This requirement of such extreme parameters naturally explains the lack of GRBs for which such a high energy component has been observed. Guetta & Granot (2003a) postulate that some GRB explosions occur inside pulsar wind bubbles. In such scenarios, afterglow electrons upscatter pulsar wind bubble photons to higher energies during the early afterglow thus producing GeV emission such as that observed in GRB 940217.

The GRB observational data are extraordinarily complex and there is no complete and definitive explanation for the diversity of properties observed. It is important to establish whether there is, in general, a VHE component of emission present during either the prompt or afterglow phase of the GRB. Understanding the nature of such emission will provide important information about the physical conditions of the emission region. One definitive observation of the prompt or afterglow emission could significantly influence our understanding of the processes at work in GRB emission and its aftermath.

In this paper, the GRBs observed with the Whipple 10 m Gamma-ray Telescope in response to HETE-2 and INTEGRAL notifications are described. The search for VHE emission is restricted to times on the order of hours after the GRB. In Section 2, the observing strategy, telescope configuration, and data analysis methods used in this paper are described. The properties of the GRBs observed and their observation with the Whipple Telescope are described in Section 3. Finally, in Section 4, the results are summarized and their implications discussed in the context of some theoretical models that predict VHE emission from GRBs. The sensitivity of future instruments such as VERITAS to GRBs is also discussed.

## 2. The Gamma-ray Burst Observations

### 2.1. Telescope Configuration

The observations presented here were made with the 10 m Gamma-ray Telescope at the Fred Lawrence Whipple Observatory. Constructed in 1968, the telescope has been operated as an IACT since 1982 (Kildea et al. in press). In September 2005, the observing program at the 10 m was redefined and the instrument was dedicated solely to the monitoring of TeV blazars and the search for VHE emission from GRBs. Located on Mount Hopkins approximately 40 km south of Tucson in southern Arizona at an altitude of 2300 m, the telescope consists of 248 hexagonal mirror facets mounted on a 10 m spherical dish with an imaging camera at its focus. The front-aluminized mirrors are mounted using the Davies-Cotton design (Davies & Cotton 1957).

The imaging camera consists of 379 photo-multiplier tubes (PMTs) arranged in a hexagonal pattern. A plate of light-collecting cones is mounted in front of the PMTs to increase their light-collection efficiency. A pattern-sensitive trigger (Bradbury & Rose 2002), generates a trigger whenever three adjacent PMTs register a signal above a level preset in the constant fraction discriminators. The PMT signals for each triggering event are read out and digitized using charge-integrating analog to digital converters. In this way, a map of the amount of charge in each PMT across the camera is recorded for each event and stored for offline analysis. The telescope triggers at a rate of  $\sim 25$  Hz (including background cosmic ray triggers) when pointing at high ( $> 50^\circ$ ) elevation. Although sensitive in the energy range from 200 GeV to 10 TeV, the peak response energy of the telescope to a Crab-like spectrum during the observations reported upon here was approximately 400 GeV. This is the energy at which the telescope is most efficient at detecting gamma rays and is subject to a 20% uncertainty.

## 2.2. Observing Strategy

Burst notifications at the Whipple Telescope for the observations described here were received via email from the Global Coordinates Network (GCN Webpage 2006). When a notification email arrived, the GRB location and time were extracted and sent to the telescope tracking control computer. An audible alarm sounded to alert the observer of the arrival of a burst notification. If at sufficient elevation, the observer approved the observations and the telescope was commanded to slew immediately to the location of the GRB. The Whipple Telescope slews at a speed of  $1^\circ \text{ s}^{-1}$  and therefore can reach any part of the visible sky within three minutes.

Seven different GRB locations were observed with the Whipple 10 m Telescope between November 2002 and April 2004. These observations are summarized in Table 1. At the time these data were taken, the point spread function of the Whipple Telescope was approximately  $0.1^\circ$  which corresponds to the field of view of one PMT. The positional offsets for the GRB observations (see Table 2) were all less than this so a conventional “point source” analysis was performed.

## 2.3. Data Analysis

The data were analyzed using the imaging technique and analysis procedures pioneered and developed by the Whipple Collaboration (Reynolds et al. 1993). In this method, each

image is first cleaned to exclude the signals from any pixels that are most likely the result of noise. The cleaned images are then characterized by calculating and storing the first, second, and third moments of the light distribution in each image. The parameters and this procedure are described elsewhere (Reynolds et al. 1993). Since gamma-ray images are known to be compact and elliptical in shape, while those generated by cosmic ray showers tend to be broader with more fluctuations, cuts can be derived on the above parameters which reject approximately 99.7% of the background images while retaining over 50% of those generated by gamma-ray showers. These cuts are optimized using data taken on the Crab Nebula which is used as the standard candle in the TeV sky.

Two different modes of observation are employed at the Whipple Telescope, “*On - Off*” and “*Tracking*” (Catanese et al. 1998). The choice of mode depends upon the nature of the target. The GRB data presented here were all taken in the *Tracking* mode. Unlike data taken in the *On - Off* mode, scans taken in the *Tracking* mode do not have independent control data which can be used to establish the background level of gamma-ray like events during the scan. These control data are essential in order to estimate the number of events passing all cuts which would have been detected during the scan in the absence of the candidate gamma-ray source. In order to perform this estimate, a tracking ratio is calculated by analyzing “darkfield data” (Horan et al. 2002). These consist of *Off-source* data taken in the *On - Off* mode and of observations of objects found not to be sources of gamma rays. A large database of these scans is analyzed and in this way, the background level of events passing all gamma-ray selection criteria can be characterized as a function of zenith angle. Since the GRB data described in this paper were taken at elevations between  $50^\circ$  and  $80^\circ$ , a large sample of darkfield data ( $\sim 233$  hours) spanning a similar zenith angle range was analyzed so that the background during the gamma-ray burst data runs could be estimated.

### 3. The Gamma-ray Bursts

This paper concentrates on the GRB observations made in response to HETE-2 and INTEGRAL triggers with the Whipple 10 m Gamma-ray Telescope; observations made in response to Swift triggers are the subject of a separate paper (Dowdall et al. in prep.). When the GRB data were filtered to remove observations made at large zenith angles, during inferior weather conditions, and of positions later reported to be the result of false triggers or to have large positional errors, the data from observations of seven GRB locations remained. These GRBs took place between UT dates 021112 and 040422; two have redshifts derived from spectral measurements, one has an estimated redshift and four lie at unknown distances. Five of the sets of GRB follow-up observations were carried out in response to

triggers from the high energy transient explorer 2 (HETE-2; Lamb et al. (2000)) while two sets of observations were triggered by the international gamma-ray astrophysical laboratory (INTEGRAL; Winkler et al. (1999)). In the remainder of this section, the properties of each of the GRBs observed and the results of these observations are presented. A summary of the GRB properties is given in Table 1 while the observations taken at the Whipple Observatory are summarized in Table 2.

### 3.1. GRB 021112

This was a long GRB with a duration of  $> 5$  s and a peak flux of  $> 3 \times 10^{-8}$  erg cm $^{-2}$  s $^{-1}$  in the 8 - 40 keV band (Ricker et al. 2002). In the 30 - 400 keV energy band, the burst had a peak energy of 57.15 keV, a duration of 6.39s and a fluence of  $2.1 \times 10^{-7}$  erg cm $^{-2}$  (MIT Webpages 2006). The triggering instrument was the French Gamma Telescope (FREGATE) instrument on HETE-2. The Milagro data taken during the time of this burst were searched for GeV/TeV gamma-ray emission. No evidence for prompt emission was found and a preliminary analysis, assuming a differential photon spectral index of -2.4, gave an upper limit on the fluence at the 99.9% confidence level of  $J(0.2 - 20 \text{ TeV}) < 2.6 \times 10^{-6}$  erg cm $^{-2}$  over a 5 second interval (McEnery et al. 2002a). Optical observations with the 0.6-meter Red Buttes Observatory Telescope beginning 1.8 hours after the burst did not show any evidence for an optical counterpart and placed a limiting magnitude of  $R_c=21.8$  (3 sigma) on the optical emission: at the time, this was the deepest non-detection of an optical afterglow within 2.6 hours of a GRB (Schaefer et al. 2002).

Two sets of observations on the location of GRB 021112 were made with the Whipple 10 m Telescope. The first observations commenced 4.2 hours after the GRB occurred and lasted for 110.6 minutes. Observations were also taken for 55.3 minutes on the following night, 28.6 hours after the GRB occurred. Upper limits (99.7% c.l.) of 0.20 Crab<sup>1</sup> and 0.30 Crab ( $E > 400$  GeV), respectively, were derived for these observations assuming a Crab-like spectrum (spectral index of -2.49).

---

<sup>1</sup>Since the Crab is the standard candle in the VHE regime, it is customary to quote upper limits as a fraction of the Crab flux at the same energy.

### 3.2. GRB 021204

Little information is available in the literature on this HETE-2 burst. The GRB location was observed with a number of optical telescopes (the RIKEN 0.2m (Torii, Yamaoka & Kato 2002), the 32 inch Tenagra II (Nysewander, Reichart & Schwartz 2002), and the 1.05 m Schmidt at Kiso Observatory (Urata et al. 2002)) but no optical transient was found to a limiting magnitude of  $R=16.5$ , 2.1 hours after the burst (Torii, Yamaoka & Kato 2002), and to  $R=18.8$ , 6.2 hours after the burst (Urata et al. 2002).

Whipple observations of this burst location commenced 16.9 hours after the GRB occurred and lasted for 55.3 minutes. An upper limit (99.7% c.l.) of 0.33 Crab was derived for the VHE emission above 400 GeV during these observations.

### 3.3. GRB 021211

This long, bright burst was detected by all three instruments on HETE-2. It had a duration  $> 5.7$  s in the 8-40 keV band with a fluence of  $\sim 10^{-6}$  erg cm $^{-2}$  during that interval (Crew 2002). The peak flux was  $> 8 \times 10^{-7}$  erg cm $^{-2}$  s $^{-1}$  (i.e.  $> 20$  Crab flux) in 5 ms (Crew 2002). This burst had a peak energy of 45.56 keV, a duration of 2.80s, and a fluence of  $2.4 \times 10^{-6}$  erg cm $^{-2}$  in the 30-400 keV energy band (MIT Webpages 2006). Fox et al. (2003) reported on the early optical, near-infrared, and radio observations of this burst. They identified a break in the optical light curve of the burst at  $t=0.1-0.2$  hr, which was interpreted as the signature of a reverse shock. The light curve comprised two distinct phases. The initial steeply-declining flash was followed by emission declining as a typical afterglow with a power-law index close to 1. KAIT observations of the afterglow also detected the steeply declining light curve and evidence for an early break (Li et al. 2003). The optical transient was detected at many observatories (Park, Williams & Barthelmy 2002; Li et al. 2002; Lamb et al. 2002; Garnavich et al. 2002a,b). The optical transient faded from an R-band magnitude of 18.3, 20.7 minutes after the burst, to an R-band magnitude of 21.1, 5.7 hours after the burst (Fox et al. 2003). Vreeswijk et al. (2002) derived a redshift of 1.006 for this burst based on spectroscopic observations carried out with the European Southern Observatory's Very Large Telescope (VLT) at Paranal, Chile. Milagro searched for emission at GeV/TeV energies over the burst duration reported by the HETE-2 wide field X-ray monitor. They did not find any evidence for prompt emission and a preliminary analysis, assuming a differential photon spectral index of -2.4, gave an upper limit on the fluence at the 99.9% confidence level of  $J(0.2-20 \text{ TeV}) < 3.8 \times 10^{-6}$  erg cm $^{-2}$  over a 6 second interval (McEnery et al. 2002b).

Whipple observations on this GRB location were initiated 20.7 hours after the GRB and lasted for 82.8 minutes. An upper limit (99.7% c.l.) on the VHE emission of 0.33 Crab ( $E > 400$  GeV) was derived from these observations.

### 3.4. GRB 030329

This GRB is one of the brightest bursts on record. It triggered the FREGATE instrument on HETE-2 in the 6 - 120 keV energy band. It had a duration 22.76 seconds, a fluence of  $1.1 \times 10^{-4}$  erg cm $^{-2}$  and a peak energy of 67.86 keV in the 30 - 400 keV band (MIT Webpages 2006). The peak flux over 1.2 seconds was  $7 \times 10^{-6}$  erg cm $^{-2}$  s $^{-1}$  which is  $> 100$  times the Crab flux in that energy band (Vanderspek et al. 2003).

The optical transient was identified by Peterson & Price (2003). Due to its slow decay (Uemura 2003) and brightness ( $R \sim 13$ ), extensive photometric observations were possible, making this one of the best-observed GRB afterglows to date. Early observations with the VLT (Greiner et al. 2003) revealed evidence for narrow emission lines from the host galaxy indicating that this GRB occurred at a low redshift of  $z=0.1687$ . Observations of the afterglow continued for many nights as it remained bright with a slow but uneven rate of decline and exhibited some episodes of increasing brightness. These observations are well-documented in the GCN archives. Spectral measurements made on 6 April 2003 by Stanek et al. (2003a) showed the development of broad peaks in flux, characteristic of a supernova. Over the next few nights, the afterglow emission faded and the features of the supernova became more prominent (Stanek et al. 2003b). These observations provided the first direct spectroscopic evidence that at least a subset of GRBs is associated with supernovae.

The afterglow was detected at many other wavelengths. Radio observations with the VLA detected a 3.5 mJy source at 8.46 GHz. This is the brightest radio afterglow detected to date (Berger, Soderberg & Frail 2003). The afterglow was also bright at submillimeter (Smith et al. 2003) and near infrared wavelengths (Lamb et al. 2003). The X-ray afterglow was detected by RXTE during a 27-minute observation that began 4 hours 51 minutes after the burst (Marshall & Swank 2003). The flux was  $\sim 1.4 \times 10^{-10}$  erg cm $^{-2}$  s $^{-1}$  in the 2 - 10 keV band ( $\sim 0.007\%$  of the Crab).

Whipple observations of the location of GRB 030329 commenced 64.6 hours after the prompt emission. In total, 241.4 minutes of observation were taken spanning five nights. The upper limits (99.7% c.l.) from each night of observation are listed in Table 2 and are displayed on the same temporal scale as the optical light curve of the GRB afterglow in

Figure 1. When these data were combined, an upper limit (99.7% c.l.) for the VHE emission above 400 GeV of 0.17 Crab was derived.

### 3.5. GRB 030501

This burst was initially detected by the imager on board the INTEGRAL satellite (IBIS/ISGRI) and was found to have a duration of  $\sim 40$  seconds (Mereghetti et al. 2003). The burst was also detected by the Ulysses spacecraft and the spectrometer instrument (SPI-ACS) on INTEGRAL (Hurley et al. 2003). Triangulation between these two detections allowed a position annulus to be computed for this GRB. As observed by Ulysses, it had a duration of  $\sim 75$  seconds and had a 25-100 keV fluence of approximately  $1.1 \times 10^{-6}$  erg cm $^{-2}$  with a peak flux of  $4.9 \times 10^{-7}$  erg cm $^{-2}$  s $^{-1}$  over 0.25 seconds. Follow-up optical observations with several telescopes did not find evidence for an optical transient (Ofek et al. 2003; Rumyantsev, Pavlenko & Pozanenko 2003a; Boer & Klotz 2003) to a limiting magnitude of  $R=18.0$ , 0.3-17 minutes after the burst (Boer & Klotz 2003) and to a limiting magnitude of  $R=20.0$ , 16.5 hours after the burst (Ofek et al. 2003).

Whipple observations of this burst location commenced 6.6 hours after its occurrence and continued for 83.1 minutes. An upper limit (99.7% c.l.) on the VHE emission ( $E > 400$  GeV) during these observations of 0.27 Crab was derived.

### 3.6. GRB 031026

This burst was located by the FREGATE instrument on HETE-2. It had a duration of 114.2 seconds with a fluence of  $2.3 \times 10^{-6}$  erg cm $^{-2}$  in the 25-100 keV energy band (Ricker et al. 2003a) while in the 30-400 keV energy band it had a duration of 31.97 s and a fluence of  $2.8 \times 10^{-6}$  erg cm $^{-2}$  (MIT Webpages 2006). Follow-up optical observations were carried out with a number of instruments including the 1.05 m Schmidt at the Kiso Observatory (Urata et al. 2003), the 32 inch Tenagra II Telescope (Nysewander et al. 2003a), and the 1.0m Telescope at the Lulin Observatory (Huang et al. 2003a), but no optical transient was found to a limiting magnitude of  $R=20.9$  for observations taken 6-12 hours after the burst (Huang et al. 2003a) and to  $I_c=20.4$  from observations taken 3.9 and 25.7 hours after the burst (Nysewander et al. 2003b). The 30m IRAM Telescope was used to search the field around the GRB location but did not detect any source with a 250 GHz flux density  $> 16$  mJy (Bertoldi et al. 2003). A spectral analysis of the prompt X-ray and gamma-ray emission from this burst revealed it to have a very hard spectrum which is unusual for such

a long and relatively faint burst (Ricker et al. 2003b). It was noted that the counts ratio of  $>1.8$  between the 7-30 keV and 7-80 keV FREGATE energy bands was one of the most extreme measured (Ricker et al. 2003a). A “new pseudo-redshift” of  $6.67 \pm 2.9$  was computed for this burst using the prescription of Pélangeon et al. (2006).

Whipple observations of this burst location were initiated 3.7 minutes after receiving the GRB notification. The burst notification however, was not received until more than 3 hours after the prompt GRB emission. Although Whipple observations commenced 3.3 hours after the prompt emission, the first data run is not included here due to inferior weather conditions. The data presented here commenced 3.7 hours after the GRB and continued for 82.7 minutes. An upper limit (99.7% c.l.) for the VHE emission ( $E > 400$  GeV) of 0.41 Crab was derived.

### 3.7. GRB 040422

This burst was detected by the imaging instrument (IBIS/ISGRI) on the INTEGRAL satellite in the 15-200 keV energy band. It had a duration of 8 seconds, a peak flux between 20 and 200 keV of  $2.7 \text{ photons cm}^{-2} \text{ s}^{-1}$  and a fluence (1 s integration time) of  $2.5 \times 10^{-7} \text{ erg cm}^{-2}$  (Gotz et al. 2003). Follow-up observations were carried out by many groups but no optical transient was detected (Malesani et al. 2003; Sonoda, Maeno & Yamauchi 2003; Rykoff 2003; Huang et al. 2003b; Piccioni et al. 2003; Rumyantsev & Pozanenko 2003b; Qiu & Hu 2003). The ROTSE-IIIb Telescope at McDonald Observatory began taking unfiltered optical data 22.1 s after the GRB. Using the first 110 s of data, a limiting magnitude of  $\sim 17.5$  was placed on the R-band emission from the GRB at this time (Rykoff 2003).

Whipple observations of this burst commenced 4.0 hours after the prompt emission and continued for 27.6 minutes. An upper limit (99.7% c.l.) on the VHE emission ( $E > 400$  GeV) of 0.62 Crab was derived.

## 4. Results and Discussion

Upper limits on the VHE emission from the locations of seven GRBs have been derived over different timescales. For each GRB, a number (1-10) of follow-up 28-minute duration observations were taken with the Whipple 10 m Telescope. These GRB data were grouped by UT day and were combined to give one upper limit for each day of observation. The limits range from 20% to 62% of the Crab flux above 400 GeV and are presented in Table 2. In addition to calculating upper limits on the GRB emission for each day, upper limits

were calculated for each of the 28-minute scans. These are plotted for each of the GRBs in Figure 2.

The usefulness of the upper limits presented here is limited by the fact that five of the GRBs occurred at unmeasured redshifts thus making it impossible to infer the effects of the infrared background light on those observations. In addition to this, the earliest observation was not made at Whipple until 3.68 hours after the prompt GRB emission. Although the Whipple 10 m Telescope is capable of beginning GRB observations less than 2 minutes after receiving notification, a number of factors, including notifications arriving during daylight and delays in the distribution of the GRB locations, delayed the commencement of the GRB observations presented here. Although data-taking for GRB 031026 began 3.7 minutes after the GRB notification was received, this notification was not distributed by the GCN until 3.3 hours after the GRB had occurred. Thus, the observations presented here cannot be used to place constraints on the VHE component of the initial prompt GRB emission and pertain only to the afterglow emission and delayed prompt emission from GRBs.

One of the main obstacles for VHE observations of GRBs is the distance scale. Pair production interactions of gamma rays with the infrared photons of the extragalactic background light attenuate the gamma-ray signal thus limiting the distance over which VHE gamma rays can propagate. Recently however, the H.E.S.S. telescopes have detected the blazar PG 1553+113 (Aharonian et al. 2006). The redshift of this object is not known but there are strong indications that it lies at  $z > 0.25$ , possibly as far away as  $z = 0.74$ . This could represent a large increase in distance to the most distant detected TeV source, revealing more of the universe to be visible to TeV astronomers than was previously thought. Although GRBs lie at cosmological distances, many have been detected at redshifts accessible to VHE observers. Of the GRBs studied here, only 2 had spectroscopic redshifts measured while the redshift of one was estimated by Pélangéon et al. (2006) using an improved version of the redshift estimator of Atteia et al. (2003). Since all of the GRBs discussed here were long bursts, it is likely that their redshifts are of order 1. Due to the unknown redshifts of most of the bursts and the uncertainty in the density of the extragalactic background light, the effects of the absorption of VHE gamma rays by the infrared background light have not been included here.

Granot, Nakar & Piran (2003) analyzed the late time light curve of GRB 030329 and find that the large variability observed at several times ( $t=1.3-1.7$  days,  $\sim 2.4-2.8$  days,  $\sim 3.1-3.5$  days and at  $\sim 4.9-5.7$  days) after the burst is most likely the result of refreshed shocks. These time intervals have been highlighted in the top panel of Figure 1 and it can be seen that some of the observations taken at Whipple occurred during these times thus imposing upper limits on the VHE emission during these refreshed shocks. Since GRB 030329

occurred at a low redshift ( $z = 0.1685$ ), it is possible that the effects of infrared absorption on any VHE emission component may not have been significant enough to absorb all VHE photons over the energy range to which Whipple is sensitive.

Figure 3 shows these scan-by-scan upper limits as a function of time since the prompt GRB emission. Also plotted are the predicted fluxes at various times after the GRB by Zhang & Mészáros (2001) and Pe’er & Waxman (2004) at  $\sim 400$  GeV, and by Guetta & Granot (2003a) at 250 GeV. Although the peak response energy of the Whipple Telescope at the time of these observations was 400 GeV, it still had sensitivity, albeit somewhat reduced, at 250 GeV.

Razzaque, Mészáros & Zhang (2004) predict a delayed GeV component in the GRB afterglow phase from the inverse-Compton up-scattering on external shock electrons. The duration of such a component is predicted to be up to a few hours, softening with time. Zhang & Mészáros (2001) investigated the different radiation mechanisms in GRB afterglows and identified parameter-space regimes in which different spectral components dominate. They found that the inverse-Compton GeV photon component is likely to be significantly more important than a possible proton synchrotron or electron synchrotron component at these high energies. The predictions of Zhang & Mészáros (2001) for VHE emission at different times after a typical “Regime II” burst are shown by squares on Figure 3. Although the observations presented here do not constrain these predictions, the sensitivity is close to that required to detect the emission predicted.

A recent analysis of archival data from the EGRET calorimeter has found a multi-MeV spectral component in the prompt phase of GRB 941017, that is distinct from the lower energy component (González et al. 2003). This high energy component appeared between 10s and 20s after the start of the GRB and had a roughly constant flux with a relatively hard spectral slope for  $\sim 200$  s. This observation is difficult to explain within the standard synchrotron model, thus indicating the existence of new phenomena. Granot & Guetta (2003) investigated possible scenarios for this high energy spectral component and found that most models fail. They concluded that the best candidate for the emission mechanism is synchrotron self-Compton emission from the reverse shock and predicted that a bright optical transient, similar to that observed in GRB 990123, should accompany this high energy component. Pe’er & Waxman (2004) explain this high energy tail as emission from the forward shock electrons in the early afterglow phase. These electrons inverse-Compton scatter the optical photons that are emitted by the reverse shock electrons resulting in powerful VHE emission for 100 s to 200 s after the burst as indicated by the lines on Figure 3. Although the observations presented here did not commence early enough after the prompt GRB emission to constrain such models, the sensitivity of the Whipple Telescope is such that the VHE

emission predicted by these models would be easily detectable for low redshift bursts.

The prediction of Guetta & Granot (2003a) for VHE emission  $5 \times 10^3$  s after the burst from the combination of external Compton emission (the relativistic electrons behind the afterglow shock upscatter the plerion radiation) and synchrotron self-Compton emission (the electrons accelerated in the afterglow emit synchrotron emission and then upscatter this emission to the VHE regime) is indicated by a star on Figure 3. The emission is predicted to have a cutoff at  $\sim 250$  GeV due to pair production of the high energy photons with the radiation field of the pulsar wind bubble. For afterglows with an external density similar to that of the inter-stellar medium, photons of up to 1 TeV are possible. It can be seen that, although the upper limits presented here are below the predicted flux from Guetta & Granot (2003a), the observations at Whipple took place after this emission was predicted to have occurred. Had data taking at Whipple commenced earlier, the emission predicted by these authors should have been detectable for nearby GRBs.

Razzaque, Mészáros & Zhang (2004) investigated the interactions of GeV and higher energy photons in GRB fireballs and their surroundings for the prompt phase of the GRB. They predict that high energy photons escaping from the fireball will interact with infrared and microwave background photons to produce delayed secondary photons in the GeV - TeV range. Although observations of the prompt phase of GRBs are difficult with IACTs since they are pointed instruments with small fields of view which must therefore be slewed to respond to a burst notification, observations in time to detect the delayed emission are possible.

There are many emission models which predict significant VHE emission during the afterglow phase of a GRB either related to the afterglow emission itself or as a VHE component of the X-ray flares that have been observed in many Swift bursts. O’Brien et al. (2006) analyzed 40 Swift bursts which had narrow-field instrument data within 10 minutes of the trigger and found that  $\sim 50\%$  had late ( $t > T_{90}$ ) X-ray flares. If the bulk of the radiation comes via synchrotron radiation as is usually supposed, then by analogy with other systems with similar properties (supernova remnants, active galactic nuclei jets), it is natural to suppose that there must also be an inverse Compton component by which photons are boosted into the GeV - TeV energy range. This process is described by Pilla & Loeb (1998) who discuss the relationship between the energy at which the high energy cutoff occurs, the bulk Lorentz factor and the size of the emission region. A high energy emission component due to inverse Compton emission has also been considered in detail for GRB afterglows by Sari & Esin (2001); the predicted flux at GeV - TeV energies is comparable to that near the peak of the radiation in the afterglow synchrotron spectrum. Only direct observations can confirm whether this is so. Guetta & Granot (2003b) predict that the  $\sim 300$  GeV photons

from the prompt GRB phase will interact with background IR photons, making delayed high energy emission undetectable unless the intergalactic magnetic fields are extremely small.

The Swift GRB Explorer has shown that  $\sim 50\%$  of GRBs have one or more X-ray flares. These flares have been detected up to  $10^5$  s ( $\sim 28$  hours) after the prompt emission (Burrows et al. 2005). Indeed, the delayed gamma-ray component detected in BATSE bursts (Connaughton 2002) may also be associated with this phenomenon. Recently, Wang, Li & Mészáros (2006) have predicted VHE emission coincident in time with the X-ray flare photons. In this model, if the X-ray flares are caused by late central engine activity, the VHE photons are produced from inverse Compton scattering of the X-ray flare photons from forward shock electrons. If the X-ray flares originate in the external shock, VHE photons can be produced from synchrotron self-Compton emission of the X-ray flare photons with the electrons which produced them. Should VHE emission be detected from a GRB coincident with X-ray flares, the time profile of the VHE emission could be used to distinguish between these two origins of the X-ray flares.

No evidence for delayed VHE gamma-ray emission was seen from any of the GRB locations observed here and upper limits have been placed on the VHE emission at various times after the prompt GRB emission. Although there are no reports of the detection of X-ray flares or delayed X-ray emission from any of these GRBs, it is likely that such emission was present in at least some of them given the frequency with which it has been detected in GRBs observed by Swift. Indeed, the light curve of GRB 030329 shows large variability amplitude a few days after the burst and, as shown in Figure 1, Whipple observations were taken during these episodes. Apart from this, a measured redshift is only available for one of the other bursts observed here and it is possible that the remaining five occurred at distances too large to be detectable in the VHE regime.

Soderberg et al. (2004) reported on an unusual GRB (GRB 031203) that was much less energetic than average. Its similarity, in terms of brightness, to an earlier GRB (GRB 980425) suggests that the nearest and most common GRB events have not been detected up until now because GRB detectors were not sensitive enough (Sazanov, Lutovinov & Sunyaev 2004). Most GRBs that have been studied up until now lie at cosmological distances. They generate a highly collimated beam of gamma rays ensuring that they are powerful enough to be detectable at large distances. Both of the less powerful GRBs detected to date occurred at considerably lower redshifts; GRB 980425 at  $z=0.0085$  and GRB 031203 at  $z=0.1055$ . Although Soderberg et al. (2004) conclude that up until now, GRB detectors have only detected the brightest GRBs and that the nearest and most common GRB events have been missed because they are less highly collimated and energetic, Ramirez-Ruiz et al. (2005) argue that the observations of GRB 031203 can indeed be the result of off-axis viewing of a

typical, powerful GRB with a jet. Should future observations prove there to be a closer, less powerful population of GRBs, these would be prime targets for IACTs.

In the past year, the Whipple Observatory 10m Telescope has been used to carry out follow-up observations on a number of GRBs detected by the Swift GRB Explorer. The analysis of these observations will be the subject of a separate paper (Dowdall et al. in prep.).

The Very Energetic Radiation Imaging Telescope Array System (VERITAS) is currently under construction at the Fred Lawrence Whipple Observatory in Southern Arizona. Two of the four telescopes are fully operational and it is anticipated that the four-telescope array will be operational by the end of 2006. GRB observations will receive high priority and, when a GRB notification is received, their rapid follow-up will take precedence over all other observations. The VERITAS Telescopes can slew at  $1^\circ \text{ s}^{-1}$  thus enabling them to reach any part of the visible sky in less than 3 minutes. When an acceptable (i.e. at high enough elevation) GRB notification is received during observing at VERITAS, an alarm sounds to alert the observer that a GRB position has arrived. Upon receiving authorization from the observer, the telescope slews immediately to the position and data-taking begins. Given that the maximum time to slew to a GRB is 3 minutes, and that Swift notifications can arrive within 30s of the GRB, it is possible that VERITAS observations could begin as rapidly as 2-4 minutes after the GRB, depending on its location with respect to the previous VERITAS target.

As has been shown above, the Whipple 10m Telescope is sensitive enough to detect the GRB afterglow emission predicted by many authors. With its improved background rejection and greater energy range, VERITAS will be significantly more sensitive for GRB observations than the Whipple 10m Telescope. The VERITAS sensitivity for observations of different durations is shown in Figure 4. Based on the assumed rate of Swift detections ( $100 \text{ year}^{-1}$ ), the fraction of sky available to VERITAS, the duty-cycle at its site and the sun avoidance pointing of Swift which maximizes its overlap with nighttime observations, it is anticipated that  $\sim 10$  Swift GRBs will be observable each year with VERITAS.

## 5. Acknowledgements

The authors would like to thank Emmet Roache, Joe Melnick, Kevin Harris, Edward Little, and all of the staff at the Whipple Observatory for their support. The authors also thank the anonymous referee for his/her comments which were very useful and improved the paper. This research was supported in part by the U. S. Department of Energy, the National Science Foundation, PPARC, and Enterprise Ireland. Extensive use was made of

the GCN web pages (<http://gcn.gsfc.nasa.gov/>). The web pages of Joachim Greiner and Stephen Holland (<http://www.mpe.mpg.de/~jcg/grbgen.html> and <http://lheawww.gsfc.nasa.gov/~sholland/grb/index.html>) proved very useful in tracking down references and information related to the GRBs discussed in this paper.

## REFERENCES

- Aharonian, F., et al. 2005, Nature (in press) astro-ph/0508073
- Aharonian, F., et al. 2006, A&A, 448, L19
- Amenomori, M., et al. 2001, AIP Conf. Proc., 558, 844
- Atkins, R., et al. 2000, ApJ, 533, L119
- Atkins, R., et al. 2004, ApJ, 604, L25
- Atkins, R., et al. 2005, ApJ, 630, 996
- Atteia, J. L., et al. 2003, astro-ph/0312371
- Berger, E., Soderberg, A. M. & Frail, D. A. 2003, GCN Circular 2014
- Bertoldi, F., et al. 2003, GCN Circular 2440
- Boer, M. & Klotz, A. 2003, GCN Circular 2224
- Boettcher, M. & Dermer, C. 1998, ApJ, 499, L131
- Bradbury, S. M. & Rose, H. J. 2002, Nucl. Instrum. Meth. A, 481, 521
- Burrows, D. N., et al. 2005, Science, 309, 1833
- Catanese, M. A., et al. 1998, ApJ, 501, 616
- Connaughton, V., et al. 1997, ApJ, 479, 859
- Connaughton, V. 2002, ApJ, 567, 1028
- Crew, G., et al. 2002, GCN Circular 1734
- Davies, J. M. & Cotton, E. S. 1957, Journal of Solar Energy, 1, 16

- Dermer, C. & Chiang, J. 1999, Proceedings of GeV - TeV Gamma-Ray Astrophysics Workshop: Toward a Major Atmospheric Cherenkov Telescope, ed. B. L. Dingus (AIP 515, New York, 2000)
- Dermer, C. & Atoyan, A. 2004, A&A, 418, L5
- Dermer, C. 2005, Proceedings of Conference “Towards a Network of Atmospheric Cherenkov Detectors VII,” 27 - 29 April, 2005, Palaiseau, France
- Dingus, B. L., Catelli, J. R. & Schneid, E. J. 1998, Proc. 4th Huntsville GRB Symposium, AIP Conf Proc, 428, 349
- Dingus, B. L., 2001, in *High Energy Gamma Ray Astronomy*, ed. F. A. Aharonian and H. J. Völk, 2001, AIP, 558, 383
- Dowdall, C., et al. (*in preparation*)
- Falcone, A. D., et al. 2006a, Proc. of the 16th Annual Astrophysics Conf. in Maryland: Gamma Ray Bursts in the Swift Era, Washington DC (astro-ph/0602135)
- Fenimore E., et al. 1999, ApJ 512, 683
- Fox, D. W., et al 2003, ApJ, 586, L5
- Fragile, P. C., Mathews, G. J., Poirier, J. & Totani, T. 2004, Astropart. Phys., 20, 591
- Galama, T. J., et al 1998, Nature, 395, 670
- Garnavich, P., et al. 2002a, GCN Circular 1750
- Garnavich, P. et al. 2002b, GCN Circular 1751
- HETE-2 pages at MIT: <http://space.mit.edu/HETE/Bursts/Data>
- Homepage of the Gamma-ray bursts Co-ordinates Network: <http://gcn.gsfc.nasa.gov>
- Gehrels, N., et al. 2004, ApJ, 611, 1005
- González, M. M., et al. 2003, Nature, 424, 749
- Gotz, D., et al. 2003, GCN Circular 2572
- Granot, J., Nakar, E. & Piran, T. 2003, Nature, 426, 138
- Granot, J. & Guetta, D. 2003, ApJ, 598, L11

- Greiner, J., et al., 2003, GCN Circular 2020
- Guetta, D. & Granot, J. 2003a, MNRAS, 340, 115
- Guetta, D. & Granot, J. 2003b, ApJ, 585, 885
- Guetta, D., et al., 2006, (in press) astro-ph/06062387
- Horan, D., et al. 2002, ApJ, 571, 753
- Huang, K., et al. 2003a, GCN Circular 2436
- Huang, K., et al. 2003b, GCN Circular 2577
- Hurley, K., et al. 1994, Nature, 372, 652
- Hurley, K., et al., 2003, GCN Circular 2187
- Kildea, J., et al., 2006, Astropart. Phys. (*in press*)
- King, A., et al., 2005, ApJ, 630, L113
- Klebesadel, R. W., Strong, I. B. & Olson, R. A. 1973, ApJ, 182, L85
- Kumar, P. & Piran, T. 2000, ApJ, 532, 286
- Lamb, D. Q., et al. 2000, AIP Conf. Proc., 522, 265-268, Ed. S. S. Holt & W. W. Zhang
- Lamb, D. Q., et al. 2002, GCN Circular 1744
- Lamb, D. Q., et al. 2003, GCN Circular 2040
- Lazzati, D., et al. 2002, A&A, 396, L5
- Lewis, D. A. 1990, Exp. Astronomy, 1, 213
- Li, W., et al. 2002, GCN Circular 1737
- Li, W., et al 2003, ApJ, 586, L9
- Lipkin, Y. M., et al. 2004, ApJ, 606, 381
- MacFadyen, A., Ramirez-Ruiz, E. & Zhang, W. 2005, American Astronomical Society Meeting, 207, 151.04 (astro-ph/0510192)
- Malesani, D., et al. 2003, GCN Circular 2573

- Mannheim, K., Hartmann, D. & Funk, B. 1996, *ApJ*, 467, 532
- Marshall, F. E. & Swank, J. H. (2003), GCN Circular 1996
- McEnery, J., et al. 2002a, GCN Circular 1724
- McEnery, J., et al. 2002b, GCN Circular 1740
- Meegan, C. A., et al. 1992, *Nature*, 355, 143
- Mereghetti, S., et al. 2003, GCN Circular 2183
- Mészáros, P. & Rees, M. J. 1993, *ApJ*, 405, 278
- Mészáros, P., Rees, M. J. & Papathanassiou, H. 1994, *ApJ*, 432, 181
- Mészáros, P. & Rees, M. J. 1994, *MNRAS*, 269, L41
- Nousek, J. A., et al. 2006, *ApJ*, 642, 389
- Nysewander, M. C., Reichart, D. & Schwartz, M. 2002, GCN Circular 1735
- Nysewander, M. C., et al. 2003a, GCN Circular 2428
- Nysewander, M. C., et al. 2003b, GCN Circular 2433
- O’Brien, P. T., et al. 2006, *ApJ* (in press), astro-ph/0601125
- Ofek, E. O., et al. 2003, GCN Circular 2201
- Padilla, L., et al. 1998, *A&A*, 337, 43
- Panateiscu, A., et al. 2006, *MNRAS* (in press), astro-ph/0508340
- Park, H. S., Williams, G. & Barthelmy, S. 2002, GCN Circular 1736
- Pe’er, A. & Waxman, E. 2004, *ApJ*, 603, L1
- Pélangéon, A., et al. 2006, Proceedings of the 16th Annual October Astrophysics Conference in Maryland, "Gamma-ray Bursts in the Swift Era", Washington DC., November 29-December 2, 2005 (astro-ph/0601150)
- Perna, R., Armitage, P. J. & Zhang, B. 2005, *ApJ*, 636, L29
- Peterson, B. A. & Price, P. A. 2003, GCN Circular 1985
- Piccioni, A., et al. 2003, GCN Circular 2578

- Pilla, R. P. & Loeb, A. 1998, *ApJ*, 494, L167
- Proga, D. & Zhang, B. 2006, *MNRAS*, 370, L61
- Qui, Y. & Hu, J. 2003, *GCN Circular* 2581
- Ramirez-Ruiz, E., et al. 2005, *ApJ*, 625, L91
- Razzaque, S., Mészáros, P. & Zhang, B. 2004, *ApJ*, 613, 1072
- Rees, M. J. & Mészáros, P. 1998, *MNRAS*, 248, 41
- Rees, M. J. & Mészáros, P. 1998, *ApJ*, 496, L1
- Reynolds, P. T., et al. 1993, *ApJ*, 404, 206
- Ricker, G., et al. 2002, *GCN Circular* 1682
- Ricker, G., et al. 2003a, *GCN Circular* 2429
- Ricker, G., et al. 2003b, *GCN Circular* 2432
- Rumyantsev, V., Pavlenko, E. & Pozanenko, A. 2003a, *GCN Circular* 2002
- Rumyantsev, V., Pavlenko, E. & Pozanenko, A. 2003b, *GCN Circular* 2580
- Rykoff, E. 2003, *GCN Circular* 2576
- Sari, R., Piran, T. & Narayan, R. 1998, *ApJ*, 497, L17
- Sari, R. & Mészáros, P. 2000, *ApJ*, 535, L33
- Sari, R. & Esin, A. A. 2001, *ApJ*, 548, 787
- Sazonov, S. Yu., Lutovinov, L. & Sunyaev, R. A. 2004, *Nature*, 429, 646
- Schaefer, J., et al. 2002, *GCN Circular* 1776
- Soderberg, A. M., et al. 2004, *Nature*, 429, 648
- Sonoda, E., Maeno, S. & Yamauchi, M. 2003, *GCN Circular* 2574
- Smith, I., et al. 2003, *GCN Circular* 2088
- Stanek, K. Z., et al. 2003a, *GCN Circular* 2107
- Stanek, K. Z., et al. 2003b, *ApJ*, 591, L17

- Torii, K., Yamaoka, H., & Kato, Y. 2002, GCN Circular 1730
- Uemura, M. 2003, GCN Circular 1989
- Urata, Y., et al. 2002, GCN Circular 1747
- Urata, Y., et al. 2003, GCN Circular 2427
- Vanderspek, R., et al. 2003, GCN Circular 1997
- Vreeswijk P., et al. 2002, GCN Circular 1785
- Wang, X. Y., Dai, Z., G & Lu, T. 2001, ApJ, 556, 1010
- Wang, X. Y., Li, Z. & Mészáros, P. 2006, ApJL (in press), astro-ph/0601229
- Winkler, C., et al. 1999, in Proc. 3<sup>rd</sup> INTEGRAL Workshop - Astro. Lett. and Communications, 29, 309
- Zhang, B. & Mészáros, P. 2001, ApJ 559, 110
- Zhang, B. & Mészáros, P. 2004, Int. J. Mod. Phys. A19 2385-2472
- Zhang, B., et al. 2006, ApJ, 642, 354

Table 1. The properties of the gamma-ray bursts described in this work.

GRB	Discovery Satellite	Trigger Number	$z$	Fluence <sup>a</sup> (erg cm <sup>-2</sup> )	T90 <sup>b</sup> (s)	Energy band (keV)
021112	HETE-2	2448	—	$2.1 \times 10^{-7}$	6.39	30 - 400
021204	HETE-2	2486	—	—	—	—
021211	HETE-2	2493	1.006 <sup>c</sup>	$2.4 \times 10^{-6}$	2.80	30 - 400
030329	HETE-2	2652	0.17 <sup>d</sup>	$1.1 \times 10^{-4}$	22.76	30 - 400
030501	INTEGRAL	596	—	$1.1 \times 10^{-6}$	$\sim 75^e$	25 - 100
031026	HETE-2	2882	6.67 <sup>f</sup>	$2.8 \times 10^{-6}$	31.97	30 - 400
040422	INTEGRAL	1758	—	— <sup>g</sup>	8 <sup>h</sup>	—

<sup>a</sup>The fluence, where available, is quoted for the energy range given in column 7 over the duration listed in column 6. For most HETE-2 bursts, this was found at: <http://space.mit.edu/HETE/Bursts/Data>.

<sup>b</sup>Except for where a footnote is referenced, the durations in this column are T90, the time interval during which 90% of the GRB photons were detected in the 30 - 400 keV energy band.

<sup>c</sup>Vreeswijk et al. (2002).

<sup>d</sup>Greiner et al. (2003).

<sup>e</sup>The fluence and duration given in the table are from burst observations with the Ulysses satellite and the SPI-ACS instrument on INTEGRAL. The event was quite weak so there is a factor of 2 uncertainty in the numbers quoted (Hurley et al. 2003). Observations with the IBIS/ISGRI instrument on INTEGRAL alone gave a duration of  $\sim 40$  seconds for the burst (Mereghetti et al. 2003).

<sup>f</sup>This redshift was determined using the redshift estimator described in Pélangéon et al. (2006).

<sup>g</sup>The fluence was not quoted for this burst over its 8 second duration. It had a fluence of  $2.5 \times 10^{-7}$  erg cm<sup>-2</sup> when integrated over 1 second (Gotz et al. 2003).

<sup>h</sup>It was not stated by Gotz et al. (2003) whether or not this duration is T90.

Table 2. The VHE GRB observations.

GRB	$T_{GRB} - T_{OBS}^a$ (hr)	Exposure (min)	Position Offset <sup>b</sup> (deg.)	$T_{GRB} - T_{UL}^c$ (hr)	Flux <sup>d</sup> (Crab)
021112	4.24	110.56	0.013	5.1	< 0.200
	28.63	55.28	0.013	29.0	< 0.303
021204	16.91	55.34	0.009	17.4	< 0.331
021211	20.69	82.79	0.058	21.9	< 0.325
030329	64.55	65.21	0.060	66.2	< 0.360
	112.58	83.17	0.022	113.8	< 0.279
	136.23	37.55	0.022	137.0	< 0.323
	162.14	27.74	0.022	162.4	< 0.519
	186.16	27.73	0.022	186.4	< 0.399
030501	6.58	83.10	0.001	7.3	< 0.265
031026	3.68	82.70	0.007	4.9	< 0.406
040422	3.99	27.63	0.062	4.2	< 0.620

<sup>a</sup>The time in hours between the start of the GRB and the beginning of observations with the Whipple 10m Telescope.

<sup>b</sup>The angular separation between the position at which these data were taken and the refined location of the GRB.

<sup>c</sup>The length of time after the GRB for which the upper limits (ULs) are quoted. Since all data are combined to compute the upper limit, the mean time of the observations is quoted as the time to which the upper limit pertains.

<sup>d</sup>This is the flux upper limit in units of equivalent Crab flux above the peak response energy of  $\sim 400$  GeV. Above this energy, the integral Crab flux is  $8.412 \pm 1.840 \times 10^{-11} \text{ cm}^{-2} \text{ s}^{-1}$ .

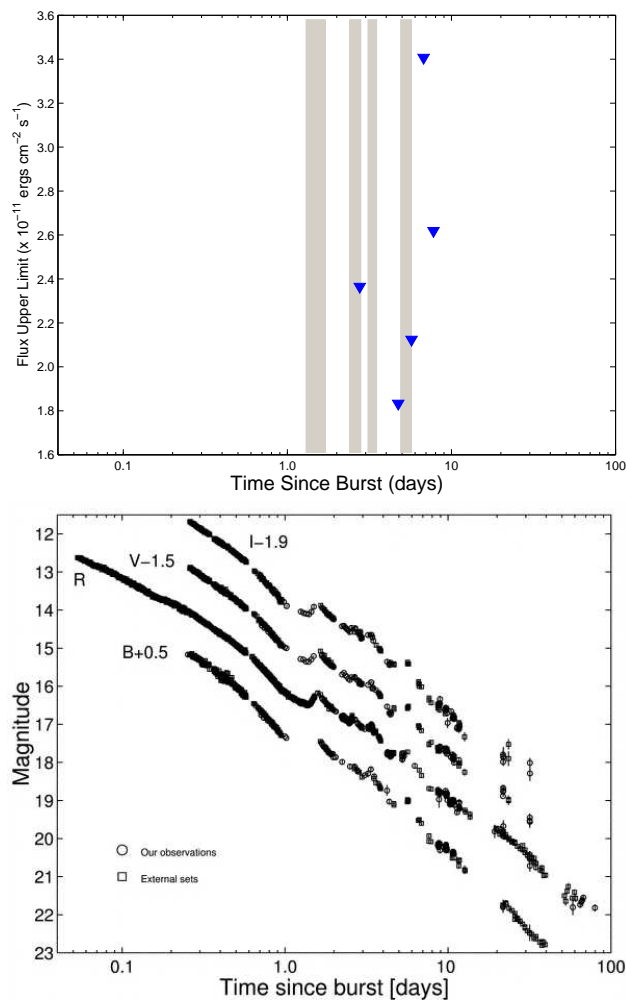


Fig. 1.— Top: The flux upper limits above 400 GeV (99.7% c.l.) on the VHE emission from GRB 030329. The time periods during which the four bumps in the lightcurve occur (Granot, Nakar & Piran 2003) are shown as shaded rectangles. Bottom: The optical light curve of GRB 030329 taken from Lipkin et al. (2004). The time since the GRB is shown with the same scale on the x-axis of both plots.

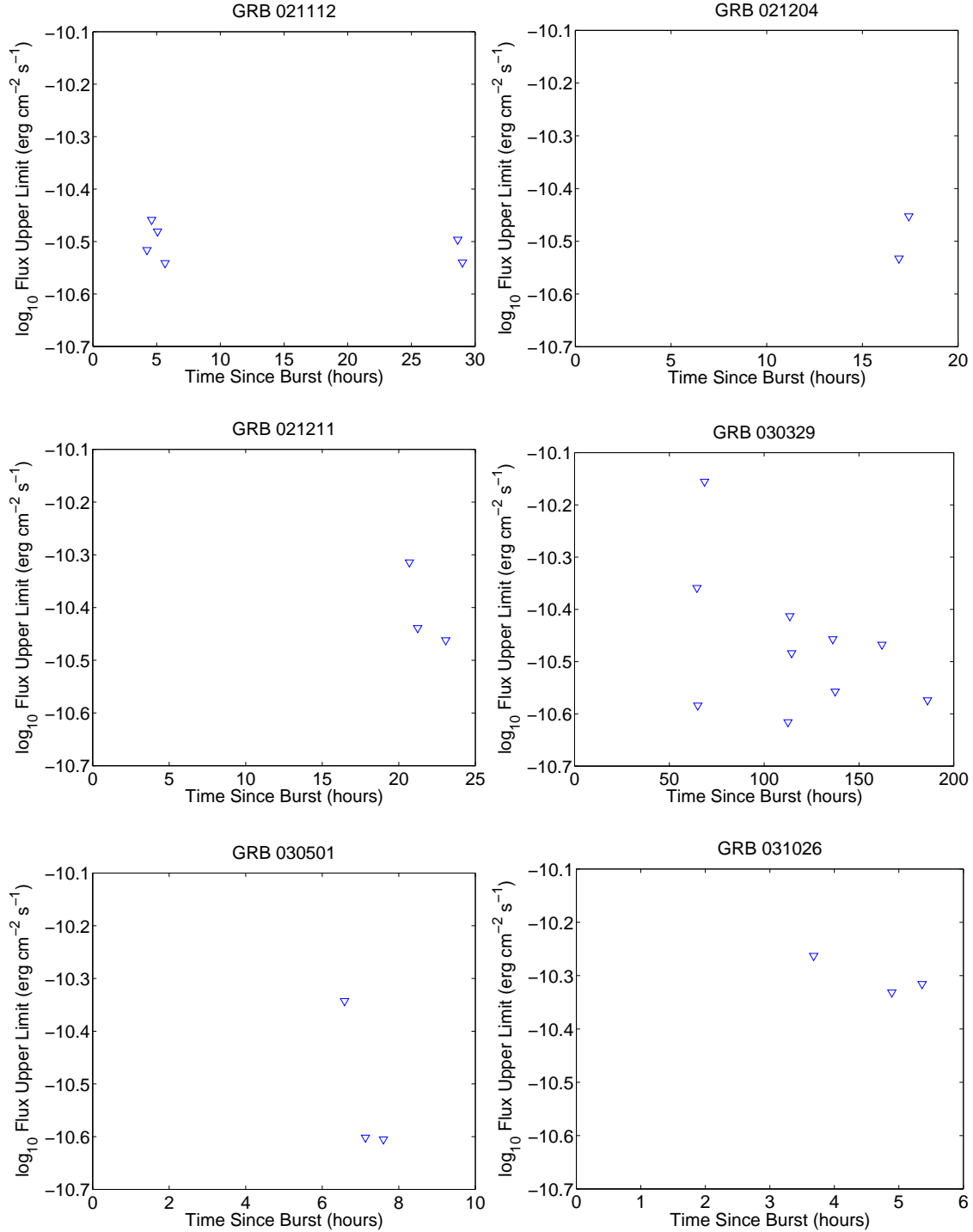


Fig. 2.— For each GRB location observed, flux upper limits in units of  $10^{-11} \text{ erg cm}^{-2} \text{ s}^{-1}$  were calculated for each 28-minute scan taken. These are plotted here as a function of the time since the GRB prompt emission for each GRB. Only one 28-minute observation was made on GRB 040422 so the plot for this GRB is not shown.

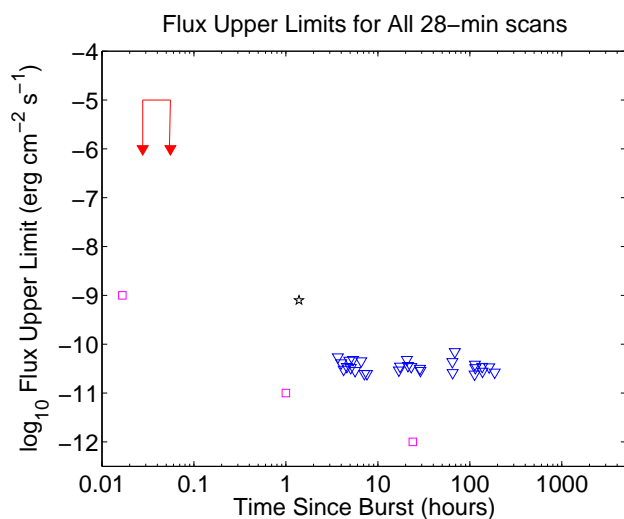


Fig. 3.— The flux upper limits above 400 GeV for all of the GRBs observed (blue triangles). The limits are plotted as a function of time since the GRB prompt emission. The approximate flux level at 400 GeV predicted by Pe’er & Waxman (2004) is indicated by the red solid lines along with the time interval during which it is predicted to occur; magenta squares show the emission at 400 GeV predicted by Zhang & Mészáros (2001) at various times after the GRB prompt emission; the prediction of Guetta & Granot (2003a) for VHE emission at 250 GeV  $5 \times 10^3$  s after the burst from the combination of external Compton and synchrotron self-Compton emission is shown by the black star.

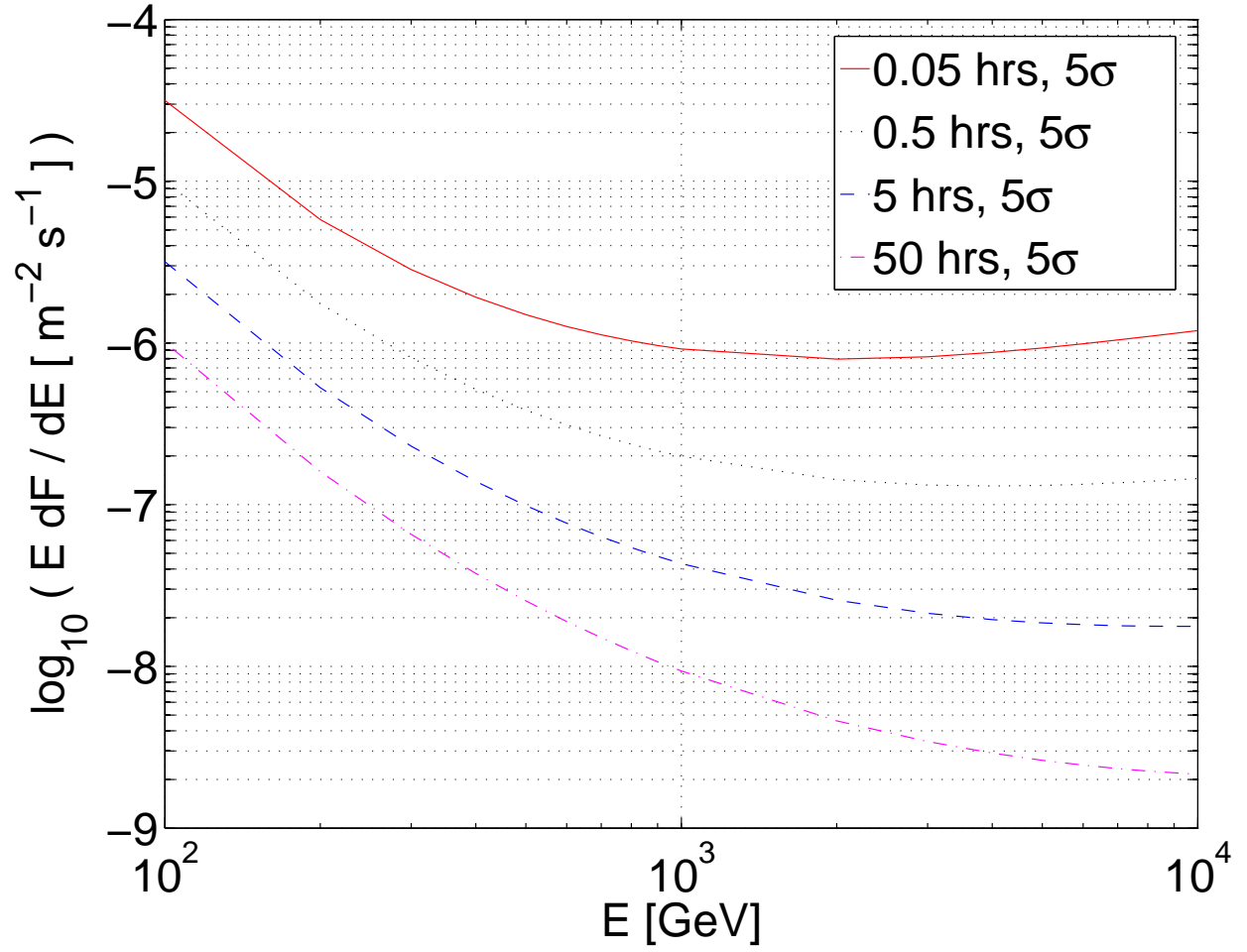


Fig. 4.— The sensitivity of the VERITAS array for exposures of 50 hours, 5 hours, 0.5 hours, and 0.05 hours (i.e., 3 minutes).